THE JOURNAL OF BIOLOGICAL CHEMISTRY VOL. 285, NO. 49, pp. 38062–38068, December 3, 2010

Timing of Gene Transcription in the Galactose Utilization System of *Escherichia coli*[*]

Received for publication, June 7, 2010, and in revised form, October 1, 2010 Published, JBC Papers in Press, October 5, 2010, DOI 10.1074/jbc.M110.152264

Péter Horváth[‡], Alexander Hunziker[§], János Erdőssy[‡], Sandeep Krishna[§], and Szabolcs Semsey[‡§1]

From the [‡]Department of Genetics, Eötvös Loránd University, H-1117 Budapest, Hungary and the [§]Center for Models of Life, Niels Bohr Institute, 2100 Copenhagen Ø, Denmark

In the natural environment, bacterial cells have to adjust their metabolism to alterations in the availability of food sources. The order and timing of gene expression are crucial in these situations to produce an appropriate response. We used the galactose regulation in *Escherichia coli* as a model system for understanding how cells integrate information about food availability and cAMP levels to adjust the timing and intensity of gene expression. We simulated the feast-famine cycle of bacterial growth by diluting stationary phase cells in fresh medium containing galactose as the sole carbon source. We followed the activities of six promoters of the galactose system as cells grew on and ran out of galactose. We found that the cell responds to a decreasing external galactose level by increasing the internal galactose level, which is achieved by limiting galactose metabolism and increasing the expression of transporters. We show that the cell alters gene expression based primarily on the current state of the cell and not on monitoring the level of extracellular galactose in real time. Some decisions have longer term effects; therefore, the current state does subtly encode the history of food availability. In summary, our measurements of timing of gene expression in the galactose system suggest that the system has evolved to respond to environments where future galactose levels are unpredictable rather than regular feast and famine cycles.

Transport and metabolism of several sugars are controlled via two feedback loops connected by a common regulator that senses the intracellular concentration of the small molecule (1, 2). The simplest systems (*e.g.* the lactose utilization system in *Escherichia coli*) consist of two operons, a regulator gene and a regulated operon containing at least two cistrons, one encoding a transporter and the other encoding an enzyme that modifies/degrades the small molecule (3). In such systems, the genes encoding the sugar transporter (*e.g. lacY*) and the enzyme for sugar degradation (*e.g. lacZ*) are regulated simultaneously. However, many sugar utilization systems reached higher levels of complexity, *e.g.* having multiple transporters, regulators, or several enzymes of a metabolic pathway. For example, the *gal* system of *E. coli* contains genes involved in the transport (*galP* and *mglBAC*) and amphibolic utilization (*galETKM*) of the sugar D-galactose. Genes of the *gal* regulon belong to different operons (4). This setup allows differential regulation of functions when needed. Regulation of the *gal* system is governed by two similar regulators, GalR and GalS, which are regulated in different ways (5–7). Previous studies suggested that GalS plays only a minor role in steady-state conditions but becomes important transiently when a high level of extracellular galactose is quickly decreased (8). Besides sensing the intracellular sugar level, galactose utilization is also regulated by the cAMP-cAMP receptor protein (CRP)[2] complex. cAMP is a signal of carbon shortage and is sensed by CRP. cAMP is synthesized intracellularly by adenylate cyclase (CyaA), which is activated when phosphorylation of Enzyme IIA^{Glc} of the phosphotransferase system is increased (9, 10). However, CyaA activity can also be regulated by a so far unknown mechanism in the presence of certain non-phosphotransferase system sugars. This mechanism does not depend on the phosphotransferase system enzymes (11, 12). Galactose availability also strongly influences the intracellular cAMP level; cells grown in a galactose-limited chemostat show substantially higher cAMP levels than cells grown in a high-galactose batch culture (13). Transcription of the galactose transport systems (GalP and MglBAC) is highly dependent on the presence of cAMP-CRP. However, transcription of the *gal* operon genes, encoding the enzymes involved in galactose utilization, occurs in both the presence and absence of cAMP-CRP when galactose is available (6). The *galETKM* operon is transcribed from two promoters, $P1_{galE}$ and $P2_{galE}$. In the absence of cAMP-CRP, $P2_{galE}$ predominantly expresses the promoter-proximal *galE* gene and very little *galK* (natural polarity), whereas in the presence of cAMP-CRP, the $P1_{galE}$ promoter expresses all of the structural genes at an equimolar level, whereas $P2_{galE}$ transcription is inhibited (14–16). Because the *galE* gene product is involved in making substrates for biosynthetic glycosylation reactions, and all of the *gal* enzymes are needed for catabolism of the sugar D-galactose, it appears that the $P2_{galE}$ transcript serves anabolic requirements, whereas transcription from $P1_{galE}$ provides for catabolism of D-galactose as a carbon source.

Proper timing of gene expression is crucial in the regulation of critical biological phenomena, *i.e.* cellular adaptation, differentiation, and development (17, 18). Biological systems evolved two fundamentally different mechanisms for the reg-

[*] This work was supported by the Hungarian Scientific Research Fund (OTKA) Grant PD75496 (to S. S.) and by the Danish National Research Foundation.

[1] To whom correspondence should be addressed: Center for Models of Life, Niels Bohr Inst., Blegdamsvej 17, 2100 Copenhagen Ø, Denmark. E-mail: semsey@nbi.dk.

[2] The abbreviations used are: CRP, cAMP receptor protein; RNAP, RNA polymerase.

ulation of timing. One possibility is that, after an initial decision, a regulatory network proceeds autonomously, executing a predefined program (18, 19). The other possibility is that the network monitors specific signals in real time and regulates timing accordingly. The goal of this work is to understand the principles governing the timing of gene expression in sugar networks when cells are grown in a batch culture containing a single sugar as a carbon source. We monitored how promoter activities in the galactose utilization network change as the cell population grows and galactose is exhausted from the medium, using specific promoter-*uidABC* (*gus*) reporter fusions. Besides responding to system-specific regulators, gene expression is also influenced by global effects, which depend on the physiological state of the cell (20–22). Because cell physiology changed in our experiments, we used a promoter that is not regulated by GalR, GalS, or cAMP-CRP as a control. On the basis of the experimental results, we built a mathematical model to calculate intracellular D-galactose and cAMP-CRP levels.

We found that intracellular reporter protein levels were higher in the stationary phase than in the early exponential phase in all cases. However, the *gal* regulon promoters differed in the timing of transcription and consequently in the timing of intracellular accumulation of the reporter proteins. Promoter activities were highly dynamic compared with intracellular reporter protein levels, which changed only 2–6-fold depending on the promoter used. We discuss how regulatory structure and signal integration logic affect timing of gene transcription.

EXPERIMENTAL PROCEDURES

Strain Construction—Regulatory regions and promoters of the *gal* regulon operons were amplified by PCR using *E. coli* MG1655 chromosomal DNA as a template (GenBank™ accession number NC_000913.2) and inserted between the EcoRI and PstI sites in plasmid pSEM2027. The amplified regulatory regions were the following: *spf* (4047775–4047954), *galR* (2974441–2974680), *galP* (3086041–3086297), the *galETKM* operon (791519 to 791214), *galS* (2239921 to 2239711), and the *mglBAC* operon (2238720 to 2238439). We used a promoter that is not regulated by cAMP-CRP or GalR as a control (GenBank™ accession number GQ872202) (23). pSEM2027 derivatives containing the cloned regulatory regions were digested with BamHI and used as a template for PCR amplification. The amplified region contained the Zeocin cassette, the *rrnBT1T2* terminators, the cloned promoter region, and part of the *gusA* ORF. This region was amplified using the "uidRZdn" (5′-ACCCGGATCCTCAATGCTGCCAGAGAGATTTTTTCAGAAAATGGATTTCACGGAATTCTCAGTCCTGCTCCTCGGCCAC-3′) and "Gusseqdn" (5′-TTCTTGTAACGCGCTTTCCCACCAAC-3′) primers. The ends of the resulting PCR fragment contained sequences of the *uid* region of the *E. coli* chromosome (50/128 bp), allowing efficient insertion using recombination-mediated genetic engineering. The PCR product was purified from an agarose gel. Recombination-mediated genetic engineering was performed according to the protocol described by Datsenko and Wanner (24). As a result, the region upstream of the *uidA* ORF, between chromosomal positions 1694107 and 1694987 (GenBank™ accession number U00096), was replaced with the synthetic construct. Recombinants were selected on LB plates containing 80 μg/ml Zeocin.

Verifying the DNA Sequence of the gal Regulatory Regions in Strains—Cells were grown overnight, and total genomic DNA was extracted using the Wizard genomic DNA purification kit (Promega). The regulatory region upstream of the *uidABC* operon was amplified by PCR (Platinum HiFi Supermix, Invitrogen) using the "KpnT1T2" (5′-ATATATGGTACCAAGCTTCTGTTTTGGCGGATGAGA-3′) and Gusseqdn primers. The DNA sequence was determined by BIOMI Ltd. (Gödöllő, Hungary).

Assay of β-Glucuronidase Activity—Cells were grown overnight in LB medium containing 100 μg/ml Zeocin and diluted 1000-fold for further growth in M63 medium containing 10 μg/ml Zeocin and supplemented with 0.4% (w/v) D-galactose, 0.1% (w/v) casamino acids (Sigma A2427), and 0.004% (w/v) vitamin B_1. At various times, aliquots of cells were removed, diluted in 1 ml of LB medium to $OD_{600} = 0.2$, pelleted, resuspended in M63 medium containing 100 μg/ml chloramphenicol, and stored at −70 °C. To determine the activity of β-glucuronidase in cells, 0.1 mg/ml lysozyme was added to 500 μl of cell suspension. After incubation for 15 min on ice, 250 μl of permeabilization buffer (100 mM Tris (pH 8), 32 mM sodium phosphate, 8 mM dithiothreitol, 8 mM CDTA, and 4% Triton X-100), containing 200 μg/ml polymyxin B (25) was added to the cell suspension. Cells were allowed to permeabilize at room temperature for 15 min before 250-μl aliquots of GUS assay buffer (0.5 mM dithiothreitol, 1 mM EDTA, and 50 mM sodium phosphate (pH 7.0)) containing 1.25 mM α-*p*-nitrophenyl-β-D-glucuronide were added. The rate of β-glucuronide hydrolysis at 37 °C was determined by measuring absorbance at 405 nm at least five different times.

Proteins—CRP was purified as described by Ryu *et al.* (26). σ^{38} was purified using the IMPACT system (New England Biolabs) as described by Shin *et al.* (27) and was mixed with the RNAP core enzyme (Epicenter) at a 1:1 molar ratio. σ^{70} RNA polymerase was purchased from U. S. Biochemical Corp.

In Vitro Transcription—Transcription reactions were performed as described previously (5). The reaction mixture (50 μl) contained 20 mM Tris acetate (pH 7.8), 10 mM magnesium acetate, 200 mM potassium glutamate, and 2 nM supercoiled DNA template. CRP was used at 50 nM and cAMP at 100 μM, when present. 20 nM RNA polymerase was added before incubating the reactions at 37 °C for 5 min. Transcription was started by the addition of 1.0 mM ATP, 0.1 mM GTP, 0.1 mM CTP, 0.01 mM UTP, and 5 μCi of [α-^{32}P]UTP (3000 Ci/mmol). Reactions were terminated after 10 min by the addition of an equal volume of transcription loading buffer (0.025% bromphenol blue, 0.025% xylene cyanol, 0.01 M EDTA, and 90% deionized formamide). After heating at 90 °C for 3 min, the samples were loaded onto urea-7% polyacrylamide DNA sequencing gels. RNA bands were quantified using the ImageQuant™ PhosphorImager (Molecular Dynamics).

Computation of Intracellular D-Galactose and cAMP-CRP Levels—Ref. 28 describes a model that takes a time series of D-Gal and cAMP-CRP levels and provides activities of P_{galR}, P_{galS}, P_{mglB}, P_{galP}, $P1_{galE}$, and $P2_{galE}$. These are further incorporated into two differential equations that compute how the levels of GalR and GalS change with time. We extended this model to include similar differential equations for the β-glucuronidase reporters for each promoter: $dP/dt = \nu_i A_i - \gamma(t)P$, where $i = P_{galR}$, P_{galE}, P_{galP}, P_{galS}, P_{mglB}, or P_{spf}. (As is the case for GalR and GalS, β-glucuronidase is assumed to be stable and diluted only by cell growth.) This model, consisting of these five differential equations in addition to the model of Ref. 28, has the following unknown parameters: the maximal production rates of β-glucuronidase under each promoter (ν_i), the time series for D-Gal, and the time series for cAMP-CRP. We varied these parameters and observed how well the resulting time series of β-glucuronidase under different promoters fitted the measured β-glucuronidase levels. We found a good fit by minimizing the least-square distance between model and observed β-glucuronidase levels using simulated annealing (29), a general algorithm for solving global optimization problems. The algorithm was implemented using C, and results were visualized in MATLAB.

RESULTS

Changes in the Reporter Protein Content of Cells Grown in a Batch Culture—Bacterial growth in batch cultures has six distinct stages: lag phase (growth rate-null), acceleration phase (growth rate increases), exponential phase (growth rate constant), retardation phase (growth rate decreases), stationary phase (growth rate-null), and the phase of decline ("death phase," growth rate-negative) (30). When diluted in fresh medium, cells first adjust their gene expression pattern to the new conditions. After this initial period, cells start to replicate, resulting in a continuous decrease in the level of available resources in the growth medium. As nutrients become limited, cells undergo an elaborate physiological and morphological differentiation to adapt to starvation. To monitor how the galactose network of *E. coli* responds when cells meet a finite pool of D-galactose in a limited volume, we created seven promoter-*uidABC* reporter fusions using the P_{galR}, P_{galE}, P_{galP}, P_{galS}, P_{mglB}, and P_{spf} promoter regions and a control promoter that is not regulated by GalR, GalS, or cAMP-CRP ("unregulated" promoter). The fusions were transferred on the chromosome of the reference strain MG1655 separately, resulting in seven strains. Strains were grown in LB medium overnight and then diluted in supplemented M63 minimal medium containing D-galactose as the sole carbon source. The level of the reporter protein (UidA = GusA) was determined at different times by measuring β-glucuronidase activities in 0.5 ml of cells diluted to $OD_{600} = 0.2$. The actual level of the reporter protein is affected by production and dilution by cell division. Therefore, for each sample measured, we recorded the optical density of the culture at 600 nm and the time counted from dilution of the culture in the minimal medium (Fig. 1).

All the reporter fusions studied behaved similarly in the sense that the intracellular β-glucuronidase level increased

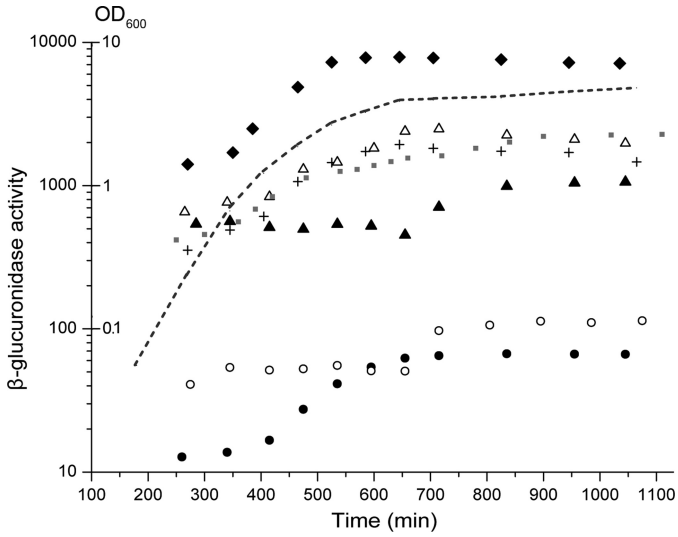

FIGURE 1. **β-Glucuronidase content of cells as a function of time.** Cells containing promoter-*uidABC* reporter fusions were grown in M63 minimal medium. At various time points, the optical density of the culture (OD_{600}) was recorded, and the β-glucuronidase enzyme activity was determined. All strains showed similar growth; therefore, only a representative growth curve is shown (*dashed line*). The β-glucuronidase activity of cells diluted to $OD_{600} = 0.2$ was plotted as a function of time for the strains containing the P_{galR} (●), P_{galE} (+), P_{galP} (△), P_{galS} (○), P_{mglB} (▲), P_{spf} (♦), and the unregulated (*gray squares*) promoter fusions. The results shown are the average of three independent measurements. S.D. was <10.6% of the mean value.

from an initial lower level to a higher level. The change was only 2–6-fold depending on the promoter used. The timing and the speed of the transition between the low and high states varied significantly for the different promoters. In four cases (*spf*, *galE*, *galP*, and *galR*), the transition occurred in the 400–600-min interval, during the shift from fast growth to very slow growth. However, in the other two cases (*galS* and *mglB*), the transition happened later, when cell doubling was almost negligible (650–800 min). In the case of the unregulated promoter, the transition between the low and high states was less sharp.

Computation of Growth Rate—From the measured OD values, we could determine how the growth rate (γ) of bacteria changed with time using the following formula: $\gamma(t) = (d/dt)\ln(\mathrm{OD}(t))$. The data show that the growth rate dropped from a maximum of 1.225 doublings/h at $t = 285$ min to a minimum of ~0.011 doublings/h at $t = 715$ min, after which the growth rate slightly increased again and then remained steady at 0.06 doublings/h until the end of the experiment. Before $t = 180$ min, we had no OD measurements, but we assume that the growth rate started at zero, remained there for a lag period of ~100 min, and then rose to its maximum at 285 min (Fig. 2*A*).

Computation of Promoter Activities—The concentration of the β-glucuronidase protein (P) in the cell is determined by the rate of protein production and by the dilution of the cell contents due to cell division. Assuming that the rate of protein production is proportional to promoter activities (A) and that the optical density of the culture (OD) is proportional to the cell number, we can calculate a time series for the promoter activities using the following equation: $A = (P_{t+\Delta t} - P_t(\mathrm{OD}_t)/\mathrm{OD}_{t+\Delta t})/\Delta T$.

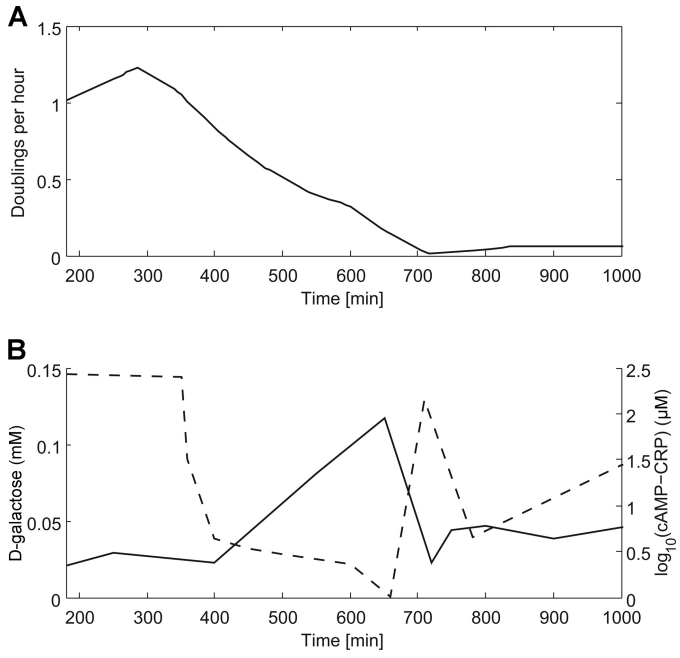

FIGURE 2. **Timing of promoter activities.** *A*, time-dependent growth rate calculated from the experiment shown in Fig. 1. *B*, intracellular cAMP-CRP and D-galactose time series as found by the simulated annealing procedure (29).

From the enzyme activity measurements of the unregulated promoter, a promoter activity time series was calculated in the same way as for the other strains. This activity, normalized to 1, was then used to scale all other promoter activities to take growth rate-dependent effects (*e.g.* gene copy/cell) and the varying resource availability (*e.g.* abundance of RNA polymerases and ribosomes) into account (Fig. 3). Unlike in previous reports using balanced growth conditions (20–22), in our experiments, the growth rate and the computed activity of the unregulated promoter did not show a direct correlation. One possible explanation for this observation is that besides production of ATP, the galactose metabolism pathway also affects other cellular processes. For example, availability of the intermediate metabolite UDP-galactose affects peptidoglycan synthesis and transcription (31).

The results show that, in the galactose system, promoter activities have different timing patterns, and the scaled activities follow two different trajectories (Fig. 3, *gray lines*). The activities of P_{galR}, P_{galE}, and P_{spf} can be characterized by a fast initial increase, followed by a sharp drop, resulting in a single peak. In the case of P_{galR} and P_{galE}, the peak is broader for the non-scaled activities. The scaled P_{galP}, P_{galS}, and P_{mglB} start expression patterns are similar, having two separate activity peaks, the first at ~250 min and the second at ~600 min for P_{galP} and 700 min for P_{galS} and P_{mglB}. The scaled and non-scaled timing patterns (Fig. 3, *gray versus black lines*) show only moderate differences, suggesting that the timing of gene expression is mostly determined by the system-specific regulators (GalR, GalS, and cAMP-CRP).

Computation of Intracellular cAMP-CRP and D-Galactose Levels—The measured promoter activities are functions of the intracellular cAMP-CRP and/or D-galactose levels and the gene expression capacity of cells. Conversely, given time series of the promoter activities, it is, in principle, possible to deduce the time development of cAMP-CRP and D-galactose. Ref. 28 describes a model that, given the intracellular cAMP-CRP and D-galactose levels, computes the activities of all *gal* regulon promoters. We used this model to find the cAMP-CRP and D-galactose time series that best fit the reporter protein activities we measured (normalized to the unregulated control to eliminate the effects of cell physiology). We found that the D-Gal level started rising significantly from $t \sim 400$ min onward, until it peaked at $t \sim 650$ min (Fig. 2*B*). After that, the level quickly decreased until $t = 720$ (the time at which the growth rate reached its minimum) before moderately increasing again. This increase is consistent with the production of the Mgl transport system at 700 min. As expected from previous observations (13), the cAMP-CRP level is inversely related to the D-Gal level; however, the biochemical background of this observation is not yet understood. The cAMP-CRP level started off high, decreasing to a low level at $t = 400$ min before rising again at $t \sim 670$ min and then dropping again when D-Gal rose at $t \sim 720$ min (Fig. 2*B*).

Changes in $P1_{galE}$ and $P2_{galE}$ Transcription—The model of Ref. 28 also enabled us to compute the relative contributions of the $P1_{galE}$ and $P2_{galE}$ promoters to galETKM transcription. We found that the main contribution to *galETKM* transcription throughout the growth curve came from $P1_{galE}$. $P2_{galE}$ rose for only a relatively short duration around the time when the cAMP-CRP level reached its minimum at $t = 670$ min (Fig. 4).

Transcription of the gal Regulon Promoters by Stationary Phase (σ^{38}) RNA Polymerase—The transition from exponential to stationary phase is accompanied by replacement of the RNA polymerase-associated σ^{70} subunit with σ^{38}, the process of which is facilitated by sequestration of σ^{70} by the Rsd protein (32). It was previously known that both the vegetative phase (σ^{70}) and stationary phase (σ^{38}) RNA polymerases can transcribe the *galETKM* operon, although they show different preferences for the $P1_{galE}$ and $P2_{galE}$ promoters (33). Our results show that the P_{mglB} promoter is active at the later stages of growth, showing ~45% of its maximal expression at 800 min. To test whether σ^{38} RNA polymerase can support transcription of P_{mglB} at a rate comparable to σ^{70} RNA polymerase, we analyzed transcription of the *gal* regulon promoters by σ^{38} and σ^{70} RNA polymerases *in vitro* in the presence and absence of cAMP-CRP (Fig. 5). Both the σ^{70} RNA polymerase (RNAP) and σ^{38} RNAP transcribed only three of the *gal* regulon promoters, $P1_{galE}$, $P2_{galE}$, and P_{galR}, in the absence of cAMP-CRP. Our results confirmed the previous observation that, as opposed to σ^{70} RNAP, σ^{38} RNAP shows strong preference for $P1_{galE}$ and transcribes $P2_{galE}$ weakly (33). Like $P2_{galE}$, P_{galR} showed lower activity when transcribed by σ^{38} RNAP compared with σ^{70} RNAP. Similar to σ^{70} RNAP transcription, cAMP-CRP activated σ^{38} RNAP transcription of $P1_{galE}$, P_{mglB}, P_{galP}, and P_{galS}. However, significant differences were obtained in the cAMP-CRP-activated levels of promoter activities. Although the σ^{38} RNAP-transcribed P_{mglB} activity reached ~70% of the transcription level obtained with σ^{70} RNAP, P_{galS} reached only ~20% (Fig. 5, *lanes 2* and *4*). Both the strong autoregulation of GalS (8) and the weak transcrip-

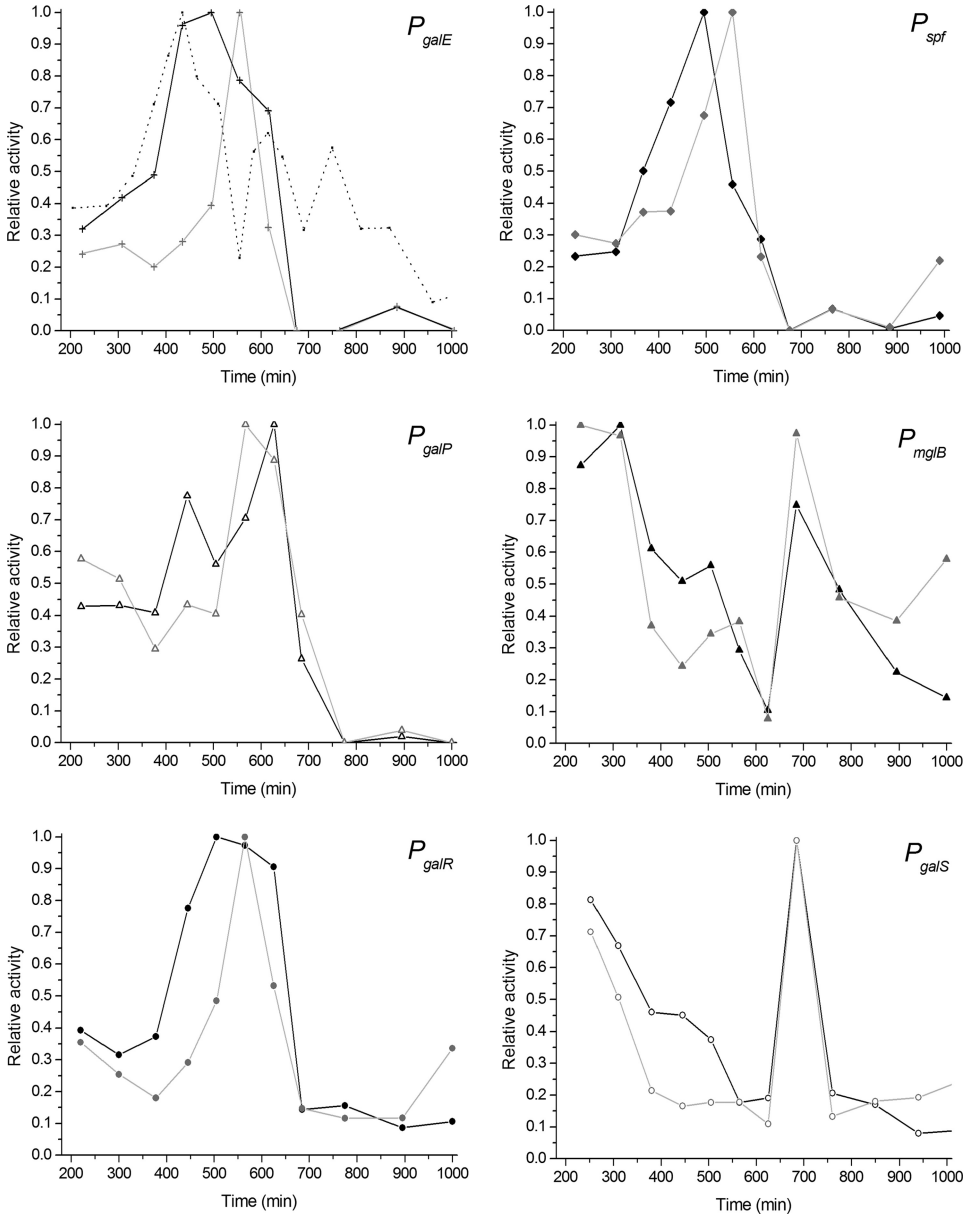

FIGURE 3. **Calculated activities of P_{galR} (●), P_{galE} (+), P_{galP} (△), P_{galS} (○), P_{mglB} (▲), and P_{spf} (♦) (*solid black lines*).** The activity of the unregulated promoter, which was used to scale all other promoter activities to take the varying resource availability into account, is shown by the *dotted line* in the *upper left panel*. The scaled activities are shown in *gray* for all promoters. Promoter activities were individually normalized to the maximal activities observed (= 1).

tion of P_{galS} by σ^{38} RNAP could explain the fast drop in P_{galS} activity (compared with P_{mglB}) between 700 and 750 min (Fig. 3). Although $P1_{galE}$ was more efficiently transcribed by σ^{38} RNAP than by σ^{70} RNAP in the absence of cAMP-CRP, σ^{38} RNAP transcription was only slightly increased compared with the activation of σ^{70} RNAP transcription in the presence of cAMP-CRP. Because the *galR* and *galS* genes are poorly transcribed by σ^{38} RNAP, we suggest that repression of the *gal* regulon promoters (primarily $P1_{galE}$ and P_{mglB}) in the stationary phase is maintained by the repressor proteins accumulated earlier.

DISCUSSION

Enteric bacteria are evolved to deal with varying nutritional conditions in nature. Nutrients are often limited in the environment (famine), but there are nutrient-rich periods as well (feast). The metabolic and morphological changes accompanying the transitions in the feast-famine cycles have been studied in detail (34). In this work, we analyzed how the galactose utilization system of *E. coli* reacts to the availability of a large but limited galactose pool. We found that galactose metabolism has a global effect on gene expression (*e.g.* through influencing nucleotide triphosphate levels) and also a specific effect on the transcription of genes belonging to the galactose regulon (through the intracellular D-galactose and cAMP levels, influencing the activity of GalR, GalS, and CRP). We computed changes in the promoter activities of the galactose regulon genes and in the intracellular D-galactose and cAMP-CRP levels. The galactose system monitors the intracellular D-galactose and cAMP-CRP levels in real time and computes

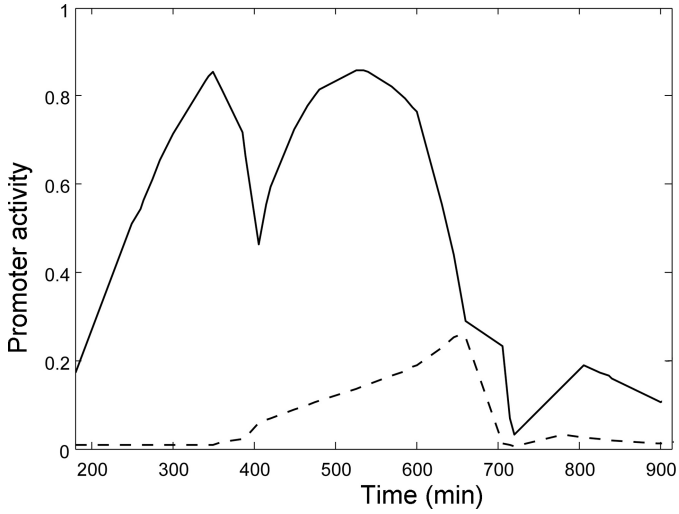

FIGURE 4. **Predicted activities of the $P1_{galE}$ (*solid line*) and $P2_{galE}$ (*dashed line*) promoters, normalized such that the maximum of the total activity is 1.**

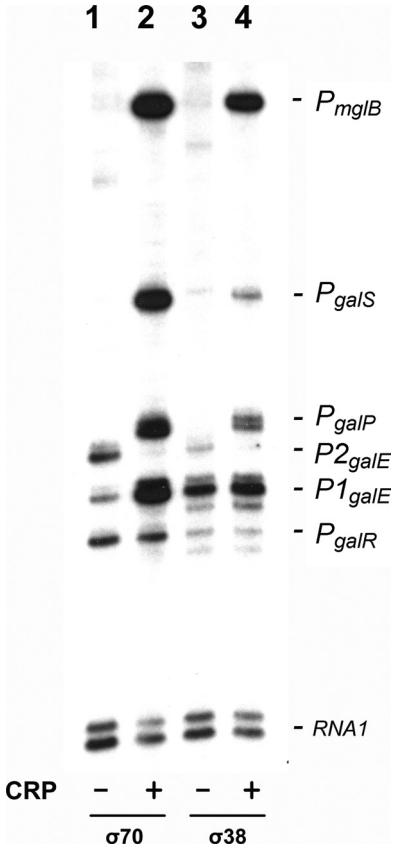

FIGURE 5. **Transcription of the *gal* regulon promoters by stationary phase (σ^{38}) RNA polymerase.** *In vitro* transcription assays were performed on a supercoiled pRPGSM DNA (6) template in the presence of the heat unstable nucleoid protein HU (80 nM) and cAMP. The presence or absence of CRP is indicated at the bottom of each lane. Experiments in *lanes 1* and *2* were performed with σ^{70} RNAP holoenzyme, and those in *lanes 3* and *4* with reconstituted σ^{38} RNAP holoenzyme.

the promoter activities accordingly. Because the proteins of the galactose system are assumed to be stable, similar to the reporter protein used, decisions of the system are limited to protein production. The actual intracellular levels of proteins depend on the history of protein production (promoter activity) and dilution (cell division). This is why promoter activities are more dynamic than protein levels. We found that timing of promoter expression depends on the current intracellular signal levels (D-Gal and cAMP-CRP), which are determined by the current extracellular galactose level and the levels of the proteins (and small RNA), affecting galactose transport and utilization (which depend on the history of the cell). Accordingly, decisions in the system are based on the current state of the cell and not on monitoring the level of extracellular galactose in real time.

Coordination of Galactose Transport and Utilization—Enzymes encoded by the *galETKM* operon are responsible for the amphibolic utilization of galactose. All of the Gal enzymes are required for galactose metabolism; however, only GalE is needed for making substrates for biosynthetic glycosylation reactions in the absence of external galactose. Transcription from the $P1_{galE}$ promoter results in equimolar expression of the Gal enzymes, serving the catabolic requirements, whereas transcription from the $P2_{galE}$ promoter results in discoordinated expression (more production of GalE and GalT than the promoter-distal GalK and GalM), which suits the biosynthetic requirements (15, 16, 35, 36). Our result that $P2_{galE}$ promoter activity is negligible when cells are grown in a galactose batch culture is consistent with this model. However, production of the proteins encoded by the *gal* operon can also be discoordinated by the Spot42 small RNA, which specifically inhibits GalK production in the absence of cAMP-CRP (37). In our experiments, transcription of the *Spot42* promoter (P_{spf}) coincided with the increase in the intracellular D-Gal level and with the decrease in the cAMP level. We suggest that inhibition of GalK production by the Spot42 small RNA is involved in balancing galactose transport and metabolism and that this regulation suits cellular needs in an environment where the extracellular galactose concentration is decreasing. Limitation in galactose transport due to the decreasing extracellular galactose concentration can be compensated by increasing the concentration of transporters. To obtain higher expression of transporters, cells need to build up a higher level of intracellular galactose, which in turn also allows increased production of the enzymes involved in galactose utilization. If the system did not reduce the rate of galactose utilization when the galactose influx decreases, the cell would quickly use up the intracellular galactose pool, leading to switching off of promoters by reactivated GalR and GalS and therefore reduced galactose transport and utilization. This effect can be overcome by changing the relative strengths of the transport and metabolism feedback loops (1). Limiting GalK production is an efficient way to block the metabolic feedback loop without compromising transport, allowing accumulation of intracellular galactose. However, Spot42 is produced at a high rate at low cAMP, regardless of whether the extracellular galactose concentration is decreasing or not. Increasing the transport capacity is likely unnecessary in a high-galactose environment; therefore, we suggest that uncoupling of the transport and metabolism loops by post-transcriptional regulation is a result of adaptation to a fluctuating galactose environment. Spot42 production allows more efficient utilization of galactose at lower extracellular concentrations, and because of the

abundance of the Spot42 small RNA, this effect can last for a few cell generations even after its synthesis is stopped (38).

In conclusion, we propose that the galactose system of *E. coli* was adapted to function in an environment where galactose levels vary in time. However, the mechanisms of decision suit environments where future galactose levels are unpredictable rather than environments with regular feast and famine cycles. If the galactose system were adapted for the latter kind of environment, with regular fluctuations, we would expect the system to give higher preference to the expression of the MglBAC transport system when the intracellular D-Gal level starts to decrease, thus avoiding the dip in the growth rate at 700 min (Fig. 2*A*).

Determinants of Transcription Patterns of Promoters in the Galactose System—Transcription of the *gal* regulon promoters (at any given time point in the experiment, shown in Fig. 1) depends on (i) the availability of resources for transcription, (ii) combinations of the intracellular cAMP and D-Gal levels, (iii) the concentration of regulators sensing these signals, and (iv) the structure and function of the regulatory region and the promoter. Previously, we described how transcription of the *gal* regulon promoters depends on cAMP and D-galactose concentrations and found that integration of the two signals at the promoters resembles Boolean logic functions (6, 28). Here, we found a correlation between the shapes of the scaled promoter activity curves (Fig. 3, *gray lines*) and the logic of signal integration at the promoters. We observed one activity peak in the case of the "D-Gal" and the "NOT cAMP" logic and two activity peaks in the case of AND-like gates (Fig. 3). However, the positions of the peaks in the latter case depend on the strength of GalR/GalS- and cAMP-CRP-binding sites in the regulatory regions. For example, for P_{galP}, which has the strongest GalR-binding sites and the highest sensitivity to cAMP-CRP activation, the second peak appears earlier compared with P_{galS}, which needs much higher cAMP-CRP levels to become activated and less D-Gal to lift GalR/GalS-mediated repression.

Acknowledgments—We thank our colleagues in the laboratory for various inputs, in particular, Thomas Soares and Mofang Liu for purification of CRP; Takácsné Botond Judit for excellent technical assistance; and Kim Sneppen, Sankar Adhya, László Orosz, Mogens H. Jensen, and András Holczinger for useful discussions and support. We also thank Hyon E. Choy for the plasmid and instructions for σ^{38} purification.

REFERENCES

1. Krishna, S., Semsey, S., and Sneppen, K. (2007) *Proc. Natl. Acad. Sci. U.S.A.* **104,** 20815–20819
2. Sneppen, K., Krishna, S., and Semsey, S. (2010) *Annu. Rev. Biophys.* **39,** 43–59
3. Monod, J., Changeux, J. P., and Jacob, F. (1963) *J. Mol. Biol.* **6,** 306–329
4. Weickert, M. J., and Adhya, S. (1993) *Mol. Microbiol.* **10,** 245–251
5. Geanacopoulos, M., and Adhya, S. (1997) *J. Bacteriol.* **179,** 228–234
6. Semsey, S., Krishna, S., Sneppen, K., and Adhya, S. (2007) *Mol. Microbiol.* **65,** 465–476
7. Weickert, M. J., and Adhya, S. (1993) *J. Bacteriol.* **175,** 251–258
8. Semsey, S., Krishna, S., Erdossy, J., Horváth, P., Orosz, L., Sneppen, K., and Adhya, S. (2009) *J. Bacteriol.* **191,** 4487–4491
9. Park, Y. H., Lee, B. R., Seok, Y. J., and Peterkofsky, A. (2006) *J. Biol. Chem.* **281,** 6448–6454
10. Reddy, P., and Kamireddi, M. (1998) *J. Bacteriol.* **180,** 732–736
11. Epstein, W., Rothman-Denes, L. B., and Hesse, J. (1975) *Proc. Natl. Acad. Sci. U.S.A.* **72,** 2300–2304
12. Hogema, B. M., Arents, J. C., Inada, T., Aiba, H., van Dam, K., and Postma, P. W. (1997) *Mol. Microbiol.* **24,** 857–867
13. Death, A., and Ferenci, T. (1994) *J. Bacteriol.* **176,** 5101–5107
14. Guidi-Rontani, C., Danchin, A., and Ullmann, A. (1984) *Mol. Gen. Genet.* **195,** 96–100
15. Lee, H. J., Jeon, H. J., Ji, S. C., Yun, S. H., and Lim, H. M. (2008) *J. Mol. Biol.* **378,** 318–327
16. Ullmann, A., Joseph, E., and Danchin, A. (1979) *Proc. Natl. Acad. Sci. U.S.A.* **76,** 3194–3197
17. Gaudet, J., Muttumu, S., Horner, M., and Mango, S. E. (2004) *PLoS Biol.* **2,** e352
18. Amir, A., Kobiler, O., Rokney, A., Oppenheim, A. B., and Stavans, J. (2007) *Mol. Syst. Biol.* **3,** 71
19. Johnson, C. H. (2004) *Curr. Issues Mol. Biol.* **6,** 103–110
20. Klumpp, S., and Hwa, T. (2008) *Proc. Natl. Acad. Sci. U.S.A.* **105,** 20245–20250
21. Klumpp, S., Zhang, Z., and Hwa, T. (2009) *Cell* **139,** 1366–1375
22. Liang, S., Bipatnath, M., Xu, Y., Chen, S., Dennis, P., Ehrenberg, M., and Bremer, H. (1999) *J. Mol. Biol.* **292,** 19–37
23. Hunziker, A., Tuboly, C., Horváth, P., Krishna, S., and Semsey, S. (2010) *Proc. Natl. Acad. Sci. U.S.A.* **107,** 12998–13003
24. Datsenko, K. A., and Wanner, B. L. (2000) *Proc. Natl. Acad. Sci. U.S.A.* **97,** 6640–6645
25. Schupp, J. M., Travis, S. E., Price, L. B., Shand, R. F., and Keim, P. (1995) *BioTechniques* **19,** 18–20
26. Ryu, S., Kim, J., Adhya, S., and Garges, S. (1993) *Proc. Natl. Acad. Sci. U.S.A.* **90,** 75–79
27. Shin, M., Song, M., Rhee, J. H., Hong, Y., Kim, Y. J., Seok, Y. J., Ha, K. S., Jung, S. H., and Choy, H. E. (2005) *Genes Dev.* **19,** 2388–2398
28. Krishna, S., Orosz, L., Sneppen, K., Adhya, S., and Semsey, S. (2009) *J. Mol. Biol.* **391,** 671–678
29. Otten, R. H. J. M., and van Ginneken, L. P. P. P. (1989) *The Annealing Algorithm*, Kluwer Academic Publishers, Boston, MA
30. Monod, J. (1949) *Annu. Rev. Microbiol.* **3,** 371–394
31. Lee, S. J., Trostel, A., Le, P., Harinarayanan, R., Fitzgerald, P. C., and Adhya, S. (2009) *Proc. Natl. Acad. Sci. U.S.A.* **106,** 19515–19520
32. Jishage, M., and Ishihama, A. (1998) *Proc. Natl. Acad. Sci. U.S.A.* **95,** 4953–4958
33. Kolb, A., Kotlarz, D., Kusano, S., and Ishihama, A. (1995) *Nucleic Acids Res.* **23,** 819–826
34. Kolter, R., Siegele, D. A., and Tormo, A. (1993) *Annu. Rev. Microbiol.* **47,** 855–874
35. Semsey, S., Virnik, K., and Adhya, S. (2006) *J. Mol. Biol.* **358,** 355–363
36. Adhya, S. (2003) *Sci. STKE.* **2003,** pe22
37. Møller, T., Franch, T., Udesen, C., Gerdes, K., and Valentin-Hansen, P. (2002) *Genes Dev.* **16,** 1696–1706
38. Mitarai, N., Benjamin, J. A., Krishna, S., Semsey, S., Csiszovszki, Z., Massé, E., and Sneppen, K. (2009) *Proc. Natl. Acad. Sci. U.S.A.* **106,** 10655–10659